 CMC, vol.38, no.2, pp.61-77, 2013

Effects of Transverse Shear on Strain Stiffening of Biological Fiber Networks

H. Jiang[1,2], B. Yang[1] and S. Liu[3]

Abstract: Actin, fibrin and collagen fiber networks are typical hierarchical biological materials formed by bundling fibrils into fibers and branching/adjoining fibers into networks. The bundled fibrils interact with each other through weak van der Waals forces and, in some cases, additional spotted covalent crosslinks. In the present work, we apply Timoshenko's beam theory that takes into account the effect of transverse shear between fibrils in each bundle to study the overall mechanical behaviors of such fiber networks. Previous experimental studies suggested that these fibers are initially loose bundles. Based on the evidence, it is hypothesized that the fibers undergo transitions from an initially loose to a tightened (due to strain effects) and finally back to a loose (due to damage) bundle under progressive loading. In correspondence, there can be identified three stages of strain stiffening and softening for the overall network deformation, consistent with results of a recent experimental in-situ neutron scattering study of fibrin networks. Finite element models are developed to examine these effects.

Keywords: fiber network, transverse shear deformation, Timoshenko's beam, bundle mechanics.

1 Introduction

A fibrin network is characterized as semiflexible, which is between a synthetic polymer network of very thin and long macromolecules and a totally stiff network of short bars (such as bridges and roofs made of trusses) [Wen and Janmey (2011)]. Since the existing theories do not apply well to such a network (including other similar semiflexible biological hierarchical networks such as those of actin and collagen), it poses a great challenge to the biomechanics community [Jahnel, Waigh

[1] Dept. of Mech. & Aerospace Engr., Univ. of Texas at Arlington, Arlington, TX 76019.
[2] Corresponding author. Email: haojiang@uta.edu; Tel: +1 817 272 1496; Fax: +1 817 272 2952
[3] State Key Laboratory of Digital Manufacturing Equipment and Technology, Huazhong University of Science and Technology, Wuhan 430074, China.

et al. (2008); Weisel (2008); Brown, Litvinov et al. (2009); Kang, Wen et al. (2009); Piechocka, Bacabac et al. (2010); Weisel (2010); Bai, Missel et al. (2011); Weigandt, Porcar et al. (2011)]. Evidently, the literature has seen a recent surge of publications attempting to interpret such experimental observations as strain stiffening that is vital to the survival of a biological system from external forces and to tackle the underlying physics [Onck, Koeman et al. (2005); Storm, Pastore et al. (2005); Buehler (2007); Chaudhuri, Parekh et al. (2007); Huisman, van Dillen et al. (2007); Janmey, McCormick et al. (2007); Lieleg, Claessens et al. (2007); Bendix, Koenderink et al. (2008); Huisman, Storm et al. (2008); Stylianopoulos, Aksan et al. (2008); Brown, Litvinov et al. (2009); Conti and MacKintosh (2009); Hatami-Marbini and Picu (2009); Kang, Wen et al. (2009); Lugovskoi, Gritsenko et al. (2009); Vader, Kabla et al. (2009); Broedersz, Kasza et al. (2010); Buell, Rutledge et al. (2010); Hudson, Houser et al. (2010); Kasza, Broedersz et al. (2010); Lindström, Vader et al. (2010); Piechocka, Bacabac et al. (2010); Bai, Missel et al. (2011); Broedersz and MacKintosh (2011); Huisman and Lubensky (2011); Piechocka, van Oosten et al. (2011); Stein, Vader et al. (2011); Kurniawan, Wong et al. (2012); Wen, Basu et al. (2012); Shayegan and Forde (2013)]. Unfortunately, many of those studies drew conclusions contradictory to one another [Weigandt, Porcar et al. (2011)].

Mesoscopic modeling and entropic elasticity have been used to describe the mechanical properties of molecules and assembly of these molecules [Storm, Pastore et al. (2005); Buehler (2006); Buehler and Wong (2007)]. In these models, the fibers were treated by using Euler-Bernoulli's beam theory where their transverse shear deformation is neglected/ignored or as a chain of beads that do not resist any shear stress at all. Stein et al. [Stein, Vader et al. (2011)] modeled collagen-I networks by adding torsional compliance at the ends of Euler-Bernoulli beams and predicted more closely to the experimental results, implying that the Euler-Bernoulli beams are too rigid for modeling these fibers. Weigandt et. al [Weigandt, Porcar et al. (2011)] recently showed, by a neutron scattering technique, interesting three stages of deformation, two stages of strain stiffening at small and large strains, respectively, and an intermediate stage of strain softening, in fibrin networks under shear. They suggested that there could be present small fibers that bear significant entropic energy for an explanation of the first stage of stiffening at small strains. The last stage of strain stiffening coincided with the fiber alignment detected by the neutron scattering measurement, which confirmed an earlier theoretical result of fiber alignment effects [Onck, Koeman et al. (2005); Huisman, van Dillen et al. (2007)]. However, it is unexplained why there occurred the intermediate stage of strain softening.

Piechocka et al. [Piechocka, Bacabac et al. (2010)] showed that the fibrin fibers ex-

hibit resistance to bending by a couple of orders of magnitude lower than what may be anticipated with their axial modulus and diameter according to Euler-Bernoulli's beam theory. They suggested that the fibrin fibers must be loose bundles of protofibrils before loading. Their entropy due to thermal vibration should be small. However, because the protofibrils are only loosely connected side-to-side, the transverse shear modulus must be small in the fibers. According to Timoshenko's beam theory, a small transverse shear modulus can throw a profound impact to the beam bending and hence characteristically change the mechanical behavior of the structure. Piechocka et al. [Piechocka, Bacabac et al. (2010)] later showed that the collagen fibers are also loose bundles of fibrils.

In the present work, Timoshenko's beam theory is applied to study the overall mechanical behavior of the hierarchical fiber networks under shear by taking into account the effects of transverse shear. The results capture two distinct stages of strain stiffening, due to tightening of initially loose bundles, which translates into an increase of transverse shear modulus, at small deformations, and due to fiber alignment at large deformations, respectively. It is also suggested that there may emerge an intermediate stage of strain softening if the crosslinks and other bonding mechanisms between fibrils in a fiber fail under high stress. The predictions are consistent with experimental results by Weigandt et al. [Weigandt, Porcar et al. (2011)]. The present analysis suggests that the effects of transverse shear in individual fibers may play a profound role in the early and intermediate stages of deformation in biological fiber networks.

The rest of the paper is organized as follows. In Sec. 2, the Timoshenko beam model is described for a fiber of bundled fibrils. In Sec. 3, the finite element model based on Timoshenko's beam theory is summarized. In Sec. 4, the finite element method is applied to examine the networks of hexagonal and triangular lattices. In Sec. 5, the results are discussed, which demonstrates a strong effect of the fiber transverse shear on the deformation of the networks. Three stages of strain stiffening and softening are suggested to interpret the recent experimental observations of Weigandt et al. [Weigandt, Porcar et al. (2011)]. In Section 6, conclusions are drawn.

2 Timoshenko Beam Model of a Bundled Fiber

Let us consider a fiber of bundled fibrils simply supported and subjected to a concentrated force at the middle point as schematically shown in Fig. 1a. The fiber is modeled as a Timoshenko beam where the transverse shear is allowed to contribute to the total deflection of the fiber. The deflection at the middle point is given as a

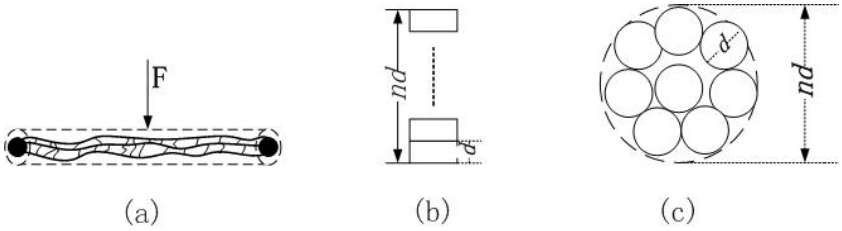

Figure 1: Schematic of a fiber of bundled fibrils with (a) a point force exerted at the middle point; (b) stack configuration; and (c) rod configuration.

sum of two terms:

$$u = u_B + u_G \tag{1}$$

$$u_B = \frac{Fl^3}{48EI} \tag{2}$$

$$u_G = \frac{\alpha Fl}{4GA} \tag{3}$$

where F is the transverse force, E, G, I, l and A are the axial Young's modulus, the transverse shear modulus, the second moment of inertia, the length and the cross-sectional area of the fiber, respectively, and α is a geometrical factor equal to 10/9 for a round and 1.2 for a square cross section. u_B and u_G are due to bending and to shear, respectively, as illustrated in Fig. 1a. The relative significance of the transverse shear is indicated by the Timoshenko factor, k_T :

$$k_T = \frac{u_G}{u_B} = \alpha \frac{12EI}{GAl^2} \tag{4}$$

The effective flexural rigidity D^* under the loading condition in Fig. 1a is defined as

$$D^* = \frac{Fl^3}{48u} = \frac{Fl^3}{48u_B}\frac{u_B}{u} = \frac{D}{1+k_T} \tag{5}$$

where D (= EI) is the flexural rigidity. It can be seen that a beam is always predicted to be more flexural by the Timoshenko theory than by the Euler-Bernoulli theory.

Further let us consider a rectangular cross section of uniformly arranged fibrils [Buehler and Wong, (2011)], as shown in Fig. 1b. Assuming that the fibrils are closely packed, the axial Young's modulus E of the fiber would be unaltered from that of the fibril. The transverse shear modulus G of the fiber is in contrast dictated

by the interfacial interaction between the fibrils. By realizing the nature of covalent bonding within individual fibrils and secondary interaction between them, it may be inferred that $E >> G$. If the (rectangular) fiber consists of n x m fibrils with n and m indicating the numbers of fibrils in the height and base directions, respectively, the flexural and shear rigidities of the fiber, D and GA, are related to those of the fibrils, D_0 and GA_0 , as

$$D = \frac{E(md)(nd)^3}{12} = mn^3 D_0 \tag{6}$$

$$GA = G(md)(nd) = mnGA_0 \tag{7}$$

Substituting Eqs. (6) and (7) in Eq. (4) yields

$$k_T = n^2 k_{T0} \tag{8}$$

where $k_{T0}(\equiv \alpha \frac{12D_0}{GA_0 l^2})$ is the Timoshenko factor as if there is only one fibril. Finally, the effective flexural rigidity of the fiber is related to the fibrils parameters as

$$D^* = \frac{mn^3 D_0}{1 + n^2 k_{T0}} \tag{9}$$

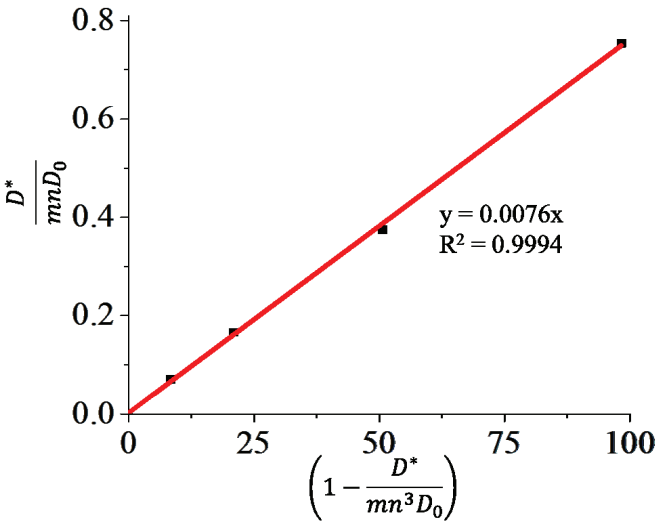

Figure 2: Variation of $\left(1 - \frac{D^*}{mn^3 D_0}\right)$ with $\frac{D^*}{mnD_0}$ for a stack of fibrils. The original data were obtained from [Buehler and Wong, (2011)].

Buehler and Wong [Buehler and Wong, (2011)] conducted a numerical experiment of collagen fibril and fiber by employing molecular dynamics simulation and obtained the fiber flexural rigidity as a function of fibril number. We took their data from Fig. 6 therein, and replotted them as $\left(1-\frac{D^*}{mn^3D_0}\right)$ vs. $\frac{D^*}{mnD_0}$ with a slope equal to k_{T0}, according to Eq. (9). As clearly shown in Fig. 2, these data fall on a straight line, resulting in $k_{T0} = 0.0076$. The value of k_{T0} is rather small relative to one unit. However, since a fibrin or collagen fiber can consist of thousands of fibrils, Eq. (9) indicates that the transverse shear effect can become significant in those situations. For the case of a circular cross section shown as Fig. 1c, the derivation process is the same and the definitions of flexural and shear rigidities will be replaced based on the change of cross section geometry.

3 Timoshenko Beam Model of a Fiber Network

Individual fibers can be modeled by using the Timoshenko beam theory. A hierarchical network is formed by joining the Timoshenko beams. Based on the Timoshenko beam theory, the transverse shear effect on the network mechanics can be captured. In this section, uniform fiber networks with hexagonal, square, and triangular unit cells are considered. As each knot in a biological fiber network usually has $3 \sim 7$ branches, a real random network can be regarded as a combination of these basic arrangements. Each fiber may consist of n fibrils and with that, the fiber thickness b is defined. All the length scales used in this model are normalized by the persistent, knot-to-knot length of the fibers. The transverse shear modulus is denoted by G_0 , which is normalized by the Young's modulus E of an individual fibril. Our objective is to find out how the overall shear modulus G of the fiber network varies with G_0 and fiber thickness b.

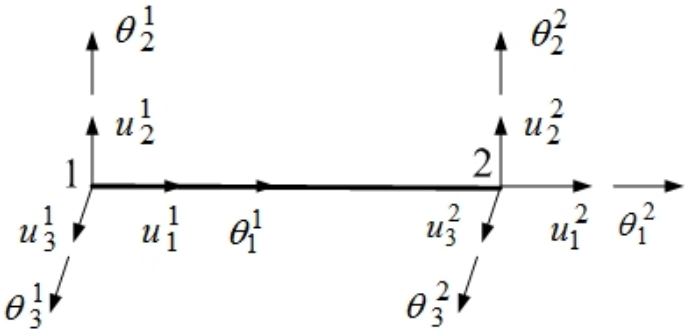

Figure 3: Schematics of a finite beam element.

The fibers in the network are discretized into initially straight finite beam elements, as shown in Fig. 3. The nodal displacements $\boldsymbol{a} = \left\{ \begin{array}{cccccc} u_1 & u_2 & u_3 & \theta_1 & \theta_2 & \theta_3 \end{array} \right\}^T$ and the nodal forces/moments $\boldsymbol{b} = \left\{ \begin{array}{cccccc} f_1 & f_2 & f_3 & m_1 & m_2 & m_3 \end{array} \right\}^T$ can be related as

$$[\boldsymbol{k}] \left\{ \begin{array}{c} \boldsymbol{a}^1 \\ \boldsymbol{a}^2 \end{array} \right\} = \left\{ \begin{array}{c} \boldsymbol{b}^1 \\ \boldsymbol{b}^2 \end{array} \right\}, \tag{10}$$

where superscripts 1 and 2 indicate either end of the element. Both $\boldsymbol{a}$ and $\boldsymbol{b}$ are measured in the local Lagrangian reference frame. The stiffness matrix $[\boldsymbol{k}]_{12\times 12}$ is symmetric and the non-zero terms in the upper triangle area are listed as follows [Cook, Malkus et al. (2001)]:

$$k_{1,1} = -k_{1,7} = k_{7,7} = \frac{EA}{L}, \tag{11a}$$

$$k_{2,2} = -k_{2,8} = k_{8,8} = \frac{12EI_Z}{(1+\varphi_Y)L^3}, \tag{11b}$$

$$k_{2,6} = k_{2,12} = -k_{6,8} = -k_{8,12} = \frac{6EI_Z}{(1+\varphi_Y)L^2}, \tag{11c}$$

$$k_{6,12} = \frac{(4+\varphi_Y)EI_Z}{(1+\varphi_Y)L}, \tag{11d}$$

$$k_{6,6} = k_{12,12} = \frac{(2-\varphi_Y)EI_Z}{(1+\varphi_Y)L}, \tag{11e}$$

$$k_{3,3} = -k_{3,9} = k_{9,9} = \frac{12EI_Y}{(1+\varphi_Z)L^3}, \tag{11f}$$

$$-k_{3,5} = -k_{3,11} = k_{5,9} = k_{9,11} = \frac{6EI_Y}{(1+\varphi_Z)L^2}, \tag{11g}$$

$$k_{5,5} = k_{11,11} = \frac{(4+\varphi_Z)EI_Y}{(1+\varphi_Z)L}, \tag{11h}$$

$$k_{5,11} = \frac{(2-\varphi_Z)EI_Y}{(1+\varphi_Z)L}, \tag{11i}$$

$$k_{4,4} = -k_{4,10} = k_{10,10} = \frac{G_0 J}{L}, \tag{11j}$$

$$\varphi_Y = \frac{12EI_Z\alpha}{AG_0L^2}, \varphi_Z = \frac{12EI_Y\alpha}{AG_0L^2}, \tag{11k}$$

where E is the axial Young's modulus, G_0 is the shear modulus within the cross-section plane, I_Y and I_Z are the moments of inertia of the cross section about the

transverse Y and Z axes, respectively, J is the polar moment of inertia, A is the cross-section area, α is the geometrical factors, and L is the element length. All of the above quantities are measured upon a body frame being continuously updated with the element over time during a simulation. It is assumed that both the linear and angular displacements in the body frame are small. By transforming the above equations to the global reference system, enforcing the equilibrium condition at each node, and transforming each quantity back to its own body frame, the following system of algebraic equations can be derived,

$$[\boldsymbol{K}] \begin{Bmatrix} \boldsymbol{a}^1 \\ \boldsymbol{a}^2 \\ \vdots \\ \boldsymbol{a}^N \end{Bmatrix} = \begin{Bmatrix} \boldsymbol{B}^1 \\ \boldsymbol{B}^2 \\ \vdots \\ \boldsymbol{B}^N \end{Bmatrix}, \tag{12}$$

where $\boldsymbol{B} = \begin{Bmatrix} F_1 & F_2 & F_3 & M_1 & M_2 & M_3 \end{Bmatrix}^T$, $\boldsymbol{F}$ and $\boldsymbol{M}$ are the external forces and moments, and $[\boldsymbol{K}]$ is the structural stiffness matrix assembled from the elemental stiffness matrix $[\boldsymbol{k}]$ over all elements; for the sake of brevity, its explicit expression is omitted.

4 Simulation Results of a Fiber Network

In this section, a rectangular sample of a hierarchical fiber network is considered, as shown in Fig. 4. Suppose that the bottom boundary of the fiber network is fixed and a shear force F is applied on the top boundary. In order to examine the unit cell configuration effects on the entire network behavior, the hexagonal, square, and triangular lattices are considered. The problem is solved by using the finite beam elements described above. The overall strain induced by the loading shear force is recorded as γ . The simulation is run for $\gamma = 0 \sim 0.6$ to examine the deformation characteristics in the low strain regime, intermediate strain regime, and high strain regime. The overall shear moduli of the fiber network during the progressive loading are calculated.

When the lattice is configured as hexagonal, each node in the lattice has three nearest neighbors. For fiber diameter-to-length ratio $b/l = 0.2$, a set of simulations are carried out with various values of transverse shear modulus, $G_0/E = 0.001$, 0.01, 0.1, 1, 10, and 100. The overall shear moduli are obtained as shown in Fig. 5(a). It can be seen that the overall shear modulus of the fiber network increases with increasing shear strain for each fixed value of transverse shear modulus G_0. In the low strain regime, the overall shear modulus increases slowly. As the loading strain increases, the overall shear modulus changes faster and reaches an approximately linear stage in the large strain regime. Also, the overall shear modulus of

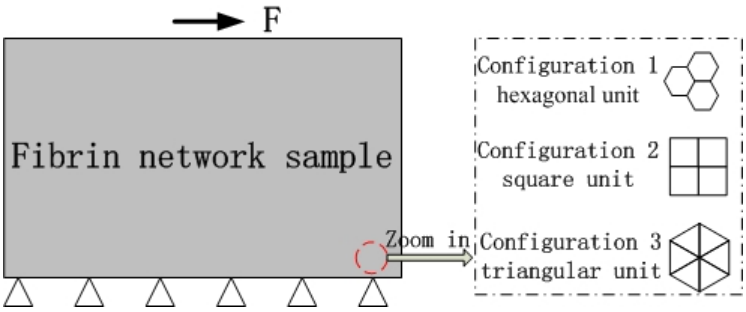

Figure 4: Loading conditions of a fiber network sample and unit cell configurations.

the fiber network apparently varies with G_0 especially when the shear modulus is small compared to the fibril Young's modulus. When the transverse shear modulus is very small such as $0.001E$, the overall shear modulus is about 0. In this case, the fibrin network can be regarded as a spring network. By increasing the transverse shear modulus G_0 , different curves of overall shear modulus are obtained. When the shear modulus changes from $10E$ to $100E$, the overall moduli are almost identical. The convergent effect implies that when the fiber transverse shear modulus is high enough, the results obtained based on Timoshenko's beam theory should be the same as the results obtained based on Euler-Bernoulli's beam theory.

Figure 5(b) shows the effects of fiber transverse shear deformability on the overall shear modulus of the network for fiber diameter-to-length ratio $b/l = 0.1$. Similar behaviors of the overall shear modulus as in Fig. 5(a) are obtained. It increases only slowly initially but more rapidly at higher strains. Eventually it increases nearly linearly. By comparing the results shown in these two figures, it can be seen that the overall effective rigidity of the network decreases with increasing fiber slenderness. When the deformation is small, the difference introduced by transverse shear modulus is relatively small. The result implies that Euler-Bernoulli's beam theory is capable to model the hierarchical fiber network approximately only when the fibers have large aspect ratios and only when the small strain regime is considered.

When the lattice is configured as square unit cell, each node in a square unit cell has four nearest neighbors. Fig. 6(a) and (b) give the results of the transverse shear modulus effects on the overall shear modulus when fiber diameter-to-length ratio $b/l = 0.1$ and 0.2, respectively. By comparing with the results of a hexagonal lattice shown in Fig. 5, it can be seen that the characteristic behavior of the network remains the same. However, with the higher number of coordination, the network becomes stiffer. Also, the network of a triangular lattice whose coordination number is six was examined, which shows the same trend of stiffening with

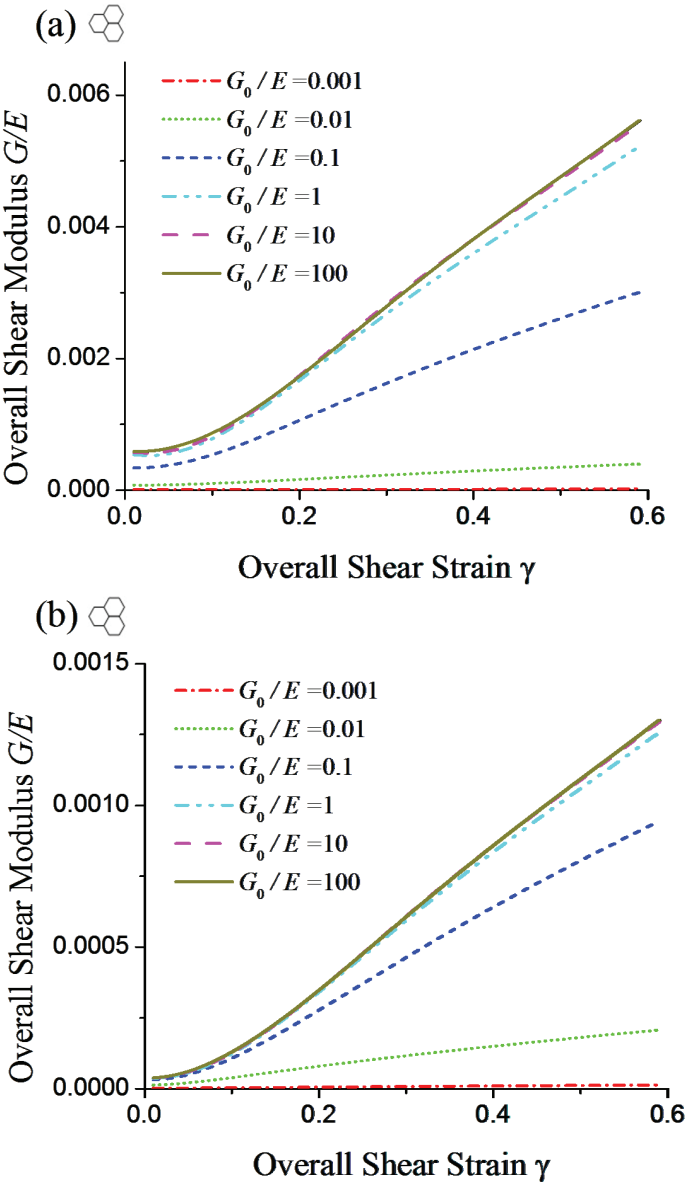

Figure 5: Variation of overall shear modulus with shear strain in a hexagonal fiber network with fiber radius to persistence length ratio b/l = (a) 0.2, (b) 0.1.

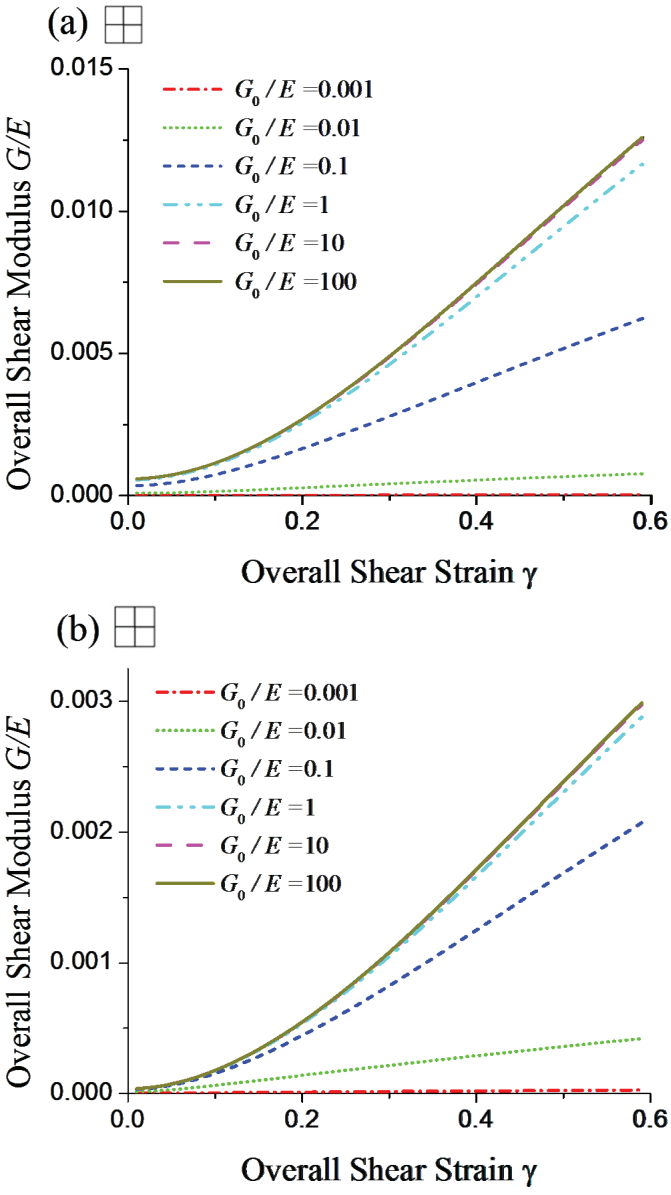

Figure 6: Variation of overall shear modulus with shear strain in a square fiber network with fiber radius to persistence length ratio b/l = (a) 0.2, (b) 0.1.

the coordination number. This trend implies that the unit cell configuration in the network would essentially change little the underlining physics.

We also calculated the bending energy and the shear deformation energy during the loading process. It is clearly shown in the calculations that the network deformation is dominantly shearing when the transverse shear modulus of fibers is small. It turns into dominantly bending when the transverse shear modulus of fibers is large.

5 Discussion

As shown in Eq. (9), the effective flexural rigidity of a fiber of bundled fibrils depends on the flexural rigidity of an individual fibril, bundled fibril number, and the Timoshenko factor. The Timoshenko factor $k_T \left(= \alpha \frac{12n^2 D_0}{GA_0 l^2}\right)$ measures the transverse shear effect on the fiber flexural rigidity. When the Timoshenko factor approaches zero, the model reduces to the Euler- Bernoulli beam theory. Equation (4) shows that the Timoshenko factor is due to the ratio of Young's modulus and transverse shear modulus E/G_0 and fiber diameter-to-length ratio b/l. If the fibril Young's modulus and the fiber aspect ratio can be held constant, the transverse shear modulus G_0 would be the only varying material parameter. When G_0 increases, the Timoshenko factor would decrease. During a progressive loading process, would G_0 vary?

Let us consider the example of a fibrin fiber. The experimental evidence suggests that a fibrin fiber is a bundle of fibrils loosely connected side-to-side [Piechocka, Bacabac et al. (2010)]. Upon loading, the bundle of fibrils would tighten up due to shear and/or axial straining. While the specific tightening mechanism is open for investigation, it is clear that the transverse shear modulus of a fibrin fiber is small before loading but increases upon loading when the bundle tightens up. The transverse shear would result in apparent bending rigidity to be lower than that of an Euler-Bernoulli beam. This bundle tightening process can manifest itself as initial stiffening of individual fibers and consequently apparent stiffening of fibrin network at small strains. At a point the fibrin fibers being bent and sheared increasingly would yield that can turn a tightened bundle back to a loose bundle. At this critical point, the fibrin fibers would lose their shear and bending resistances and become chain- or rope-like that can only sustain axial tensile loading. This may cause the network to apparently soften temporarily. Upon the transformation, the hierarchical network essentially becomes a network of linear springs. At higher loading, the fibrin fibers would align themselves with the loading direction, resulting in another stage of strain stiffening [Onck, Koeman et al. (2005); Huisman, van Dillen et al. (2007)].

According to the above understanding, one may expect the overall shear modu-

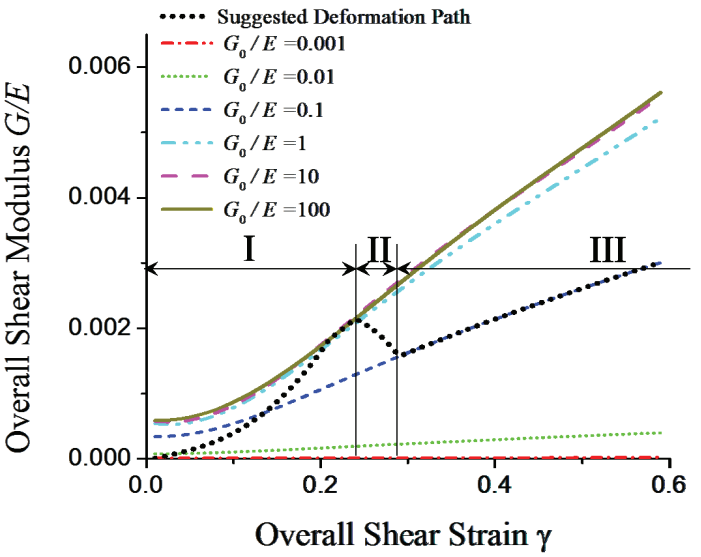

Figure 7: Suggested deformation path in a realistic fibrin network experiencing strain stiffening due to tightening of bundled fibrils (stage I), strain softening due to damage (stage II), and strain stiffening again (due to fiber alignment).

lus to follow the dark dotted line with increasing strain during a shear experiment [Weigandt, Porcar et al. (2011)], as shown in Fig. 7. The bunch of reference curves are for fixed values of G_0/E copied from Fig. 5a. The dark dotted curve navigates among these curves with evolving G_0/E as discussed above.

When the fiber is not stretched, the shear modulus between fibrils in such a loose bundle is at a low level. Let us suppose that the fiber internal shear modulus starts at $0.001E$. When the fiber is stretched, the distance between fibril in the fiber gets smaller and the bundle becomes firmer, which implies an increase of the transverse shear modulus. This is the first strain stiffening phase, depicted as stage I in Fig. 7. In this phase, the strain stiffening effect is due to tightening of initially loose bundles. It can be seen that the overall effective shear modulus climbs up across the contour lines with increasing transverse shear modulus. When the overall strain continues to increase, the bundle is tightened and the overall effective shear modulus reaches the highest level, say, the line of G_0/E = 100. At this point, the fiber behaves like an Euler-Bernoulli beam, and the overall shear modulus saturates with any further increase of G_0/E. However, as the loading continues to rise, the fibrin fiber will reach its yielding point. As discussed above, the fibrin fibers would lose

their ability to resist shear and bending, and this event manifests itself as an abrupt decrease of transverse shear modulus, marked as stage II in Fig. 7. During this phase, the overall shear modulus drops/softens. As the loading rises further, the weakened fibers align themselves with the loading direction. This alignment effect has been understood to apparently stiffen the network, depicted as stage III in Fig. 7. These understandings are consistent with experimental results by Weigandt et al. [Weigandt, Porcar et al. (2011)].

It may be worth noting that if the crosslinks are strong enough to survive the loading before the fiber alignment effect emerges, the intermediate strain softening stage may not be observed. The behavior of overall shear modulus depends on the competition between the decreasing effect due to the transverse shear yielding of each fiber and the increasing effect induced by the fiber alignment. Possible buckling of some fibers in the network may also contribute to the decrease of overall shear modulus of the network.

6 Conclusion

Timoshenko's beam theory that takes into account the effects of transverse shear is applied to study the overall mechanical behavior of a general hierarchical fiber networks under shear. A uniform lattice consist of connected beams is used to model the fibrin network for demonstration. By subjecting a shear loading on the lattice, we ran calculations of the model with finite deformation effects taken into account. The overall shear moduli of the network represented by unit cells with various symmetries for various values of transverse shear modulus are plotted. The results show the overall shear modulus of a hierarchical fiber network is apparently changed with the values of transverse shear modulus. By analyzing the mechanism of a loose bundle, a deformation path of the network is suggested that captures the two strain stiffening stages due to the tightening of initially loose bundles and the fiber alignment, respectively. A possible intermediate stage of strain softening due to the crosslinks and/or other bonding mechanisms between fibrils failing under high shear stress is also considered that explains well the experimental observation [Weigandt, Porcar et al. (2011)].

Reference

Bai, M.; Missel, A. R.; Levine, A. J.; Klug, W. S. (2011): On the role of the filament length distribution in the mechanics of semiflexible networks. *Acta biomaterialia,* vol. 7, no. 5, pp. 2109-2118.

Bendix, P. M.; Koenderink, G. H.; Cuvelier, D.; Dogic, Z.; Koeleman, B. N.; Brieher, W. M.; Field, C. M.; Mahadevan, L.; Weitz, D. A. (2008): A quanti-

tative analysis of contractility in active cytoskeletal protein networks. *Biophysical Journal,* vol. 94, no. 8, pp. 3126-3136.

Broedersz, C. P.; Kasza, K. E.; Jawerth, L. M.; Münster, S.; Weitz, D. A.; MacKintosh, F. C. (2010): Measurement of nonlinear rheology of cross-linked biopolymer gels. *Soft Matter*, vol. 6, no. 17, pp. 4120.

Broedersz, C. P.; MacKintosh, F. C. (2011): Molecular motors stiffen non-affine semiflexible polymer networks. *Soft Matte*r, vol. 7, no. 7, pp 3186.

Brown, A. E.; Litvinov, R. I.; Discher, D. E.; Purohit, P. K.; Weisel, J. W. (2009): Multiscale Mechanics of Fibrin Polymer: Gel Stretching with Protein Unfolding and Loss of Water. *Science*, vol. 325, no. 5941, pp. 741-744.

Buehler, M. J. (2006): Atomistic and continuum modeling of mechanical properties of collagen: Elasticity, fracture, and self-assembly. *Journal of Materials Research*, vol. 21, no. 08, pp. 1947-1961.

Buehler, M. J. (2007): Nano- and micromechanical properties of hierarchical biological materials and tissues. *Journal of Materials Science*, vol. 42,no. 21, pp. 8765-8770.

Buehler, M. J.; Wong, S. Y. (2007): Entropic elasticity controls nanomechanics of single tropocollagen molecules. *Biophysical Journal*, vol. 93, no. 1, pp. 37-43.

Buell, S.; Rutledge, G. C.; Vliet, K. J. V. (2010): Predicting polymer nanofiber interactions via molecular simulations. *ACS Applied Materials & Interfaces*, vol. 2, no. 4, pp. 1164-1172.

Chaudhuri, O.; Parekh, S. H.; Fletcher, D. A. (2007): Reversible stress softening of actin networks. *Nature*, vol. 445, no. 7125, pp.295-298.

Conti, E.; MacKintosh, F. (2009): Cross-Linked Networks of Stiff Filaments Exhibit Negative Normal Stress. *Physical Review Letters*, vol. 102, no. 8, pp. 088102.

Cook, R. D.; Malkus, D. S.; Plesha, M. E.; Witt, R. J. (2001): *Concepts and Applications of Finite Element Analysis*, Wiley.

Hatami-Marbini, H.; Picu, R. C. (2009): Effect of fiber orientation on the non-affine deformation of random fiber networks. *Acta Mechanica*, vol. 205, no. 1-4, pp. 77-84.

Hudson, N. E.; Houser, J. R.; O'Brien III, E. T.; Taylor II, R. M.; Superfine, R.; Lord, S. T.; Falvo, M. R. (2010): Stiffening of Individual Fibrin Fibers Equitably Distributes Strain and Strengthens Networks. *Biophysical Journal*, vol. 98, no.8, pp. 1632-1640.

Huisman, E.; Lubensky, T. (2011): Internal Stresses, Normal Modes, and Non-affinity in Three-Dimensional Biopolymer Networks. *Physical Review Letters*, vol. 106, no.8, pp. 088301.

Huisman, E.; Storm, C.; Barkema, G. T. (2008): Monte Carlo study of multiply crosslinked semiflexible polymer networks. *Physical Review E*, vol. 78, no. 5, pp. 051801.

Huisman, E. M.; Dillen, T. V.; Onck, P. R.; Giessen, E. V. D. (2007): Three-Dimensional Cross-Linked F-Actin Networks: Relation between Network Architecture and Mechanical Behavior. *Physical Review Letters*, vol. 99, no. 20, pp. 208103.

Jahnel, M.; Waigh, T. A.; Lu, J. R. (2008): Thermal fluctuations of fibrin fibres at short time scales. *Soft Matter*, vol. 4, no. 7, pp. 1438.

Janmey, P. A.; McCormick, M. E.; Rammensee, S.; Leight, J. L.; Georges, P. C.; MacKintosh, F. C. (2007): Negative normal stress in semiflexible biopolymer gels. *Nature Materials*, vol. 6, no. 1, pp. 48-51.

Kang, H.; Wen, Q.; Janmey, P. A.; Tang, J. X.; Conti, E.; MacKintosh, F. C. (2009): Nonlinear Elasticity of Stiff Filament Networks: Strain Stiffening, Negative Normal Stress, and Filament Alignment in Fibrin Gels. *Journal of Physical Chemistry B*, vol. 113, no. 12, pp. 3799-3805.

Kasza, K. E.; Broedersz, C. P.; Koenderink, G. H.; Lin, Y. C.; Messner, W.; Millman, E. A.; Nakamura, F.; Stossel, T. P.; MacKintosh, F. C.; Weitz, D. A. (2010): Actin filament length tunes elasticity of flexibly cross-linked actin networks. *Biophysical Journal*, vol. 99, no. 4, pp. 1091-1100.

Kurniawan, N. A.; Wong, L. H.; Rajagopalan, R. (2012). Early stiffening and softening of collagen: interplay of deformation mechanisms in biopolymer networks. *Biomacromolecules*, vol. 13, no. 3, pp. 691-698.

Lieleg, O.; Claessens, M. M.; Heussinger, C.; Frey, E.; Bausch, A. R. (2007): Mechanics of Bundled Semiflexible Polymer Networks. *Physical Review Letters*, vol. 99, no.8, pp. 088102..

Lindström, S. B.; Vader, D. A.; Kulachenko, A.; Weitz, D. A. (2010): Biopolymer network geometries: Characterization, regeneration, and elastic properties. *Physical Review E*, vol. 82, no. 5, pp. 051905.

Lugovskoi, E. V.; Gritsenko, P. G.; Komisarenko, S. V. (2009): Molecular mechanisms of the polymerization of fibrin and the formation of its three-dimensional network. *Russian Journal of Bioorganic Chemistry*, vol. 35, no. 4, pp. 393-410.

Onck, P. R.; Koeman, T.; Van Dillen, T.; Van der Giessen, E. (2005): Alternative Explanation of Stiffening in Cross-Linked Semiflexible Networks. *Physical Review Letters*, vol. 95, no. 17, pp. 178102.

Piechocka, I. K.; Bacabac, R. G.; Potters, M.; MacKintosh, F. C.; Koenderink, G. H. (2010): Structural Hierarchy Governs Fibrin Gel Mechanics. *Biophysical*

Journal, vol. 98, no. 10, pp. 2281-2289.

Piechocka, I. K.; van Oosten, A. S.; Breuls, R. G.; Koenderink, G. H. (2011): Rheology of heterotypic collagen networks. *Biomacromolecules*, vol. 12, no. 7, pp. 2797-2805.

Shayegan, M.; Forde, N. R. (2013). Microrheological characterization of collagen systems: from molecular solutions to fibrillar gels. *PloS one*, vol. 8, no. 8, pp. e70590.

Stein, A. M.; Vader, D. A.; Weitz, D. A.; Sander, L. M. (2011): The micromechanics of three-dimensional collagen-I gels. *Complexity*, vol. 16, no. 4, pp. 22-28.

Storm, C.; Pastore, J. J.; MacKintosh, F. C.; Lubensky, T. C.; Janmey, P. A. (2005): Nonlinear elasticity in biological gels. *Nature*, vol. 435, no.7039, pp. 191-194.

Stylianopoulos, T.; Aksan, A.; Barocas, V. H. (2008): A structural, kinetic model of soft tissue thermomechanics. *Biophysical Journal*, vol. 94, no. 3, pp. 717-725.

Vader, D.,; Kabla, A.; Weitz, D.; Mahadevan, L. (2009): Strain-Induced Alignment in Collagen Gels. *PloS one*, vol. 4, no. 6, pp. e5902.

Weigandt, K. M.; Porcar, L.; Pozzo, D. C. (2011): In situ neutron scattering study of structural transitions in fibrin networks under shear deformation. *Soft Matter*, vol. 7, no. 21, pp. 9992.

Weisel, J. W. (2008): Biophysics. Enigmas of blood clot elasticity. *Science*, vol. 320, no. 5875, pp. 456-457.

Weisel, J. W. (2010): Biomechanics in hemostasis and thrombosis. *Journal of thrombosis and haemostasis : JTH*, vol. 8, no. 5, pp. 1027-1029.

Wen, Q.; Basu, A.; Janmey, P. A.; Yodh, A. G. (2012): Non-affine deformations in polymer hydrogels. *Soft matter*, vol. 8, no. 31, pp. 8039-8049.

Wen, Q.; Janmey, P. A. (2011): Polymer physics of the cytoskeleton. *Current Opinion in Solid State and Materials Science*, vol. 15, no. 5, pp. 177-182.